

Gene Expression Profiling in Clinically Localized Prostate Cancer: A Four-Gene Expression Model Predicts Clinical Behavior

Alain Latil,¹ Ivan Bièche,^{2,3} Laurent Chêne,¹
Ingrid Laurendeau,² Philippe Berthon,¹
Olivier Cussenot,^{4,5,6} and Michel Vidaud²

¹UroGene, Génomole, Evry cedex; ²Laboratoire de Génétique Moléculaire–Unité Propre de Recherche et d’Enseignement Supérieur Equipe Associée 3618, Faculté des Sciences Pharmaceutiques et Biologiques de Paris, Paris; ³Laboratoire d’Oncogénétique Institut National de la Santé et de la Recherche Médicale E0017, Centre René Huguenin, St. Cloud; ⁴Département d’Urologie, Université Paris VII, Hôpital Saint-Louis, Paris; ⁵Institut Universitaire de France, Paris; and ⁶Centre de Recherche pour les Pathologies Prostatiques Equipe Associée 3104, Faculté de Médecine, Paris, France

ABSTRACT

Purpose: New diagnostic and prognostic molecular markers are required for prostate cancer, one of the most common male malignancies in Western countries. Gene expression profiling may help to identify genes involved in prostate carcinogenesis, yield clinical biomarkers, and improve tumor classification.

Experimental Design: To identify fundamental differences between normal and neoplastic prostate tissue, we used real-time quantitative RT-PCR assays to quantify the mRNA expression of 291 selected genes in samples of normal prostate and of well-documented primary, clinically localized prostate tumors.

Results: Forty-six genes showed significantly different expression in tumors relative to normal prostate. The dysregulated genes belong notably to the extracellular membrane and extracellular membrane remodeling categories and are involved in angiogenesis. Furthermore, we obtained a four-gene (*XLKDI/LYVE1*, *CGA*, *F2R/PARI*, and *BCL-G*) model that discriminated between the seven patients with and the seven patients without relapse, independently of stage and grade.

Conclusions: Some dysregulated genes are good candidates for use as molecular markers and/or therapeutic targets. Furthermore, differential gene expression profiling of clinically localized prostate tumors from relapsing and non-relapsing patients identified a set of four genes with a pattern of expression that defines a molecular signature that could predict the clinical behavior of this disease.

Received 2/24/03; revised 7/22/03; accepted 7/22/03.

The costs of publication of this article were defrayed in part by the payment of page charges. This article must therefore be hereby marked *advertisement* in accordance with 18 U.S.C. Section 1734 solely to indicate this fact.

Requests for reprints: Dr. Alain Latil, UroGene, 4 rue Pierre Fontaine, F-91058, Evry cedex, France. Phone: 33-1-60-87-89-75; Fax: 33-1-60-87-89-89; E-mail: a.latil@urogene.com.

INTRODUCTION

CaP⁷ is one of the most common malignancies and the second cause of cancer death among Western men (1). Its morbidity and mortality in the growing elderly population makes CaP a major public health problem. Treatment is ineffective in advanced stages, and the disease must, therefore, be diagnosed early, when the tumor is still confined to the prostate and can be eradicated by radical prostatectomy. Early diagnosis of CaP is currently based on a combination of digital rectal examination and PSA assay and is confirmed by biopsy. However, these tests lack sensitivity, and radical prostatectomy carries a substantial risk of incontinence and impotence. Moreover, about one-third of men who undergo radical prostatectomy for localized tumors relapse, and this risk cannot be accurately predicted by using available markers (clinical stage, serum PSA level, Gleason score, pathological stage, and the number of positive biopsies). New diagnostic and prognostic markers and new therapeutic targets are urgently needed.

The initiation and progression of CaP involves multiple changes in gene expression. cDNA microarray technology offers the possibility of comparing the expression of large numbers of genes between normal and malignant tissues and was recently used to identify disease-related gene expression patterns in prostate samples (2–4). Discrepancies among reported CaP gene expression signatures could be attributable to the fact that prostate tumors contain many cell types, in addition to carcinoma cells, such as epithelial cells, stroma cells, endothelial cells, adipose cells, and infiltrating lymphocytes. cDNA microarray studies require abundant starting material, and neoplastic epithelial cells cannot be precisely microdissected from their normal counterparts. In addition, although cDNA microarrays can be used to compare the mRNA expression of thousands of genes analyzed in parallel, they cannot discriminate between gene clusters with a high degree of homology (*e.g.*, p14, p15, and p16 on chromosome arm 9p). Finally, cDNA microarrays cannot reveal small variations in gene expression or changes in important but weakly expressed genes (*e.g.*, *CYP19* and *hTERT* in prostate tumors).

To circumvent the technical problems inherent in the cDNA microarray technique, we used a quantitative real-time RT-PCR assay that is a reference in terms of its performance, accuracy, sensitivity, wide dynamic range, and high throughput capacity for nucleic acid quantification.

In this study, we applied RT-PCR to 291 selected genes involved in pathways (*e.g.*, cell cycling, signal transduction, apoptosis, angiogenesis, and metastasis) that are known to be

⁷ The abbreviations used are: CaP, prostate cancer; Ct, threshold cycle; PSA, prostate-specific antigen; ROC, receiver operating characteristic; AUC, area(s) under the curve; ECM, extracellular membrane; MMP, matrix metalloproteinase;

Extracellular matrix		Signal transduction		Transcription factors	
CLDN4	Claudin 4	APC	Adenomatosis polyposis coli	BRCA1	Breast cancer 1, early onset
COL1A1	Collagen, type I, alpha 1	ARHA	Rho A	BRCA2	Breast cancer 2, early onset
COL1A2	Collagen, type I, alpha 2	ARHC	Rho C	CEBPA	CCAAT/enhancer binding prot.a
FN1	Fibronectin 1	AXIN1	Axin	E2F1	E2F transcription factor 1
HAS2	Hyaluronan synthase 2	BCAR1	Cas	JUN	jun proto-oncogene
HPSE	Heparanase	CAV1	Caveolin 1	JUNB	jun B proto-oncogene
KAI1	kangai 1	CAV2	Caveolin 2	UND	jun D proto-oncogene
PLG	Plasminogen	CD9	CD9 antigen (p24)	MYC	c-Myc oncogene
SDC1	Syndecan 1	CDC42	Cell division cycle 42	NKX3A	NK3 transcription factor homolog A
SPARC	Secreted prot. acidic cyst-rich	CHG1L	Chromosome condensation 1-like	SNAI1	Snail homolog 1
SPARCL1	SPARC-like 1 (Hevin)	CTNNA1	Catenin alpha 1	SNAI2	Snail homolog 2 (SLUG)
THBS1	Thrombospondin-1	CTNNB1	Catenin beta 1	TCF1	Hepatic nuclear factor 1 (HNF1)
VTN	Vitronectin	FYN	FYN oncogene	TCF4	Transcription factor 4
Matrix proteases		Growth factors			
MMP2	Matrix metalloproteinase 2	GRB2	Growth factor bound protein	AREG	Amphiregulin
MMP7	Matrix metalloproteinase 7	HMG1	High mobility group 1	AS3	androgen-induced prostate associated protein
MMP9	Matrix metalloproteinase 9	HRAS	H-Ras oncogene	BMP2	Bone morphogenetic protein 2
MMP14	MT1-MMP	ILK	Integrin-like kinase	BMP4	Bone morphogenetic protein 4
PLAT	Plasminogen activator, tissue	IQGAP1	IQ GTPase activator 1	BMP6	Bone morphogenetic protein 6
PLAU	Plasminogen activator, urokinase	IQGAP2	IQ GTPase activator 2	BMP7	Bone morphogenetic protein 7
Inhibitors of matrix proteases				CGA	Glycoprot. hormone alpha polypeptide
SERPINB1	Serine proteinase inhibitor (PAI1)	KIS	Kinase interacting gene	CTGF	Connective tissue growth factor
SERPINB2	Serine proteinase inhibitor (PAI2)	MADH4	Mothers against decapentaplegic homolog 4	EGF	Epidermal growth factor
TIMP1	Tissue inhibitor 1 of MMP	MAPK4	Mitogen-activated protein kinase 4	EREG	Epiregulin
TIMP2	Tissue inhibitor 2 of MMP	MUC1	Mucin 1	FGF2	Fibroblast growth factor 2
TIMP3	Tissue inhibitor 3 of MMP	NF1	Neurofibromin	FGF7	Fibroblast growth factor 7
TIMP4	Tissue inhibitor 4 of MMP	NF2	Neurofibromin 2 Merlin	FST	Follistatin
Cell adhesion and cell junction		NRAS	N-Ras oncogene	GRO1	Gro1 oncogene
ANXA6	Annexin A6	PAK1	p21/CDC42/RAC1 activated kinase1	GRP	Gastrin-releasing peptide
GJA1	Connexin 43	PIK3CA	PI3K catalytic p110 alpha	HGF	Hepatocyte growth factor
GJA5	Connexin 40	PIK3R1	PI3K p85 alpha subunit	IFNG	Interferon, gamma
GJB1	Connexin 32	PIM1	Pim-1 oncogene	IGF2	Insulin-like growth factor 2
GJB2	Connexin 26	PLA2G1B	Phospholipase A2, group IB	IGFBP2	IGF binding protein 2
DSG2	Desmoglein 2	PRKCA	Protein kinase C alpha	IL1A	Interleukin 1, alpha
CDH1	E-Cadherin	PRNP	Prion protein 2	IL6	Interleukin 6
CD44	Hyaluronan receptor (CD44 Ag)	PTEN	Phosphatase and tensin homolog	IL10	Interleukin 10
HMMR	Hyaluronan receptor (RHAMM)	PTK2	Focal adhesion kinase (FAK)	INSL6	Insulin-like 6
ITGA2	Integrin a1	RAB13	RAB13, member RAS oncogene family	KISS1	Kiss-1 metastasis-suppressor
ITGA1	Integrin a2	RAC1	Rac 1	KITLG	Stem cell factor
ITGA5	Integrin a5	RAF1	Raf oncogene	NRG1	Neuregulin 1
ITGA6	Integrin a6	RAI3	Retinoic acid induced 3	NRG2	Neuregulin 2
ITGAV	Integrin aV	RASA1	GTPase activating protein 1	NRG3	Neuregulin 3
ITGB1	Integrin b1	ROCK1	Rho-associated protein K 1	NTN1	Netrin 1
ITGB3	Integrin b3	SHC1	Shc transforming protein	PDGFA	PDGF alpha chain
ITGB4	Integrin b4	SOS1	Sos protein	PDGFB	PDGF beta chain (Sis)
Cytoskeletal		SRC	SRC oncogene	RLN1	Relaxin 1
ACTN4	Actinin, alpha 4	SSI-1	Suppressor cytokine sig.1 (SOCS1)	SDF1	CXC chemokine ligand 12 (CXCL12)
CALD1	Caldesmon 1	SSPN	K-Ras oncogene	SLIT1	Slit homolog 1
KRT19	Keratine 19	STMN1	Stathmin 1 / Oncoprotein 18	SLIT2	Slit homolog 2
MAPT	Microtubule-associated protein tau	STMN2	Stathmin-like 2	SLIT3	Slit homolog 3
TIAM1	T-cell lymphoma invasion metastasis	STMN3	Stathmin-like 3	TGFA	Transforming growth factor, alpha
TMSB4X	Thymosin beta 4	VIL2	Villin 2 (Ezrin/EMR)	TGFB1	Transforming growth factor beta 1
Nuclear receptors		Cell cycle		TGFB2	Transforming growth factor beta 2
AR	Androgen receptor	ARF	p19/AKT protein	TNF	Tumor necrosis factor
ESR1	Estrogen receptor 1	ATM	Ataxia telangiectasia mutated		
ESR2	Estrogen receptor 2	CCND1	Cyclin D1		
PPARG	Peroxisome prolif activ Receptor g	CCNE1	Cyclin E1		
PGR	Progesterone receptor	CDKN1B	CDK inhibitor 1B, p27 protein		
RARA	Retinoic acid receptor alpha	CDKN2A	CDK inhibitor, p16 protein		
RXRA	Retinoic X receptor alpha	CDKN2B	CDK inhibitor, p15 protein		
THRA	Thyroid hormone receptor alpha	GADD45A	GADD45 alpha		
THRB	Thyroid hormone receptor beta	MAD2L1	Mitotic arrest deficiente like 1		
		MDM2	Mdm2 protein		
		MKI67	Proliferation-related Ki-67 antigen		
		TOP2A	Topoisomerase II alpha		
		RB1	Retinoblastoma		
		SFN	Stratifin		

Fig. 1 List of the selected genes.

disregulated in solid tumors, including CaP (Fig. 1). We studied 14 clinically localized prostate tumors from well-documented sources and 7 normal prostate tissues. Our aim was to identify new candidate diagnostic and prognostic markers and therapeutic targets.

MATERIALS AND METHODS

Patients and Samples

Primary prostate tumor samples were obtained from patients undergoing prostate surgery at St. Louis Hospital (Paris),

La Cavale Blanche Hospital (Brest), and Nancy University Hospital, France.

Clinically localized tumors were removed by radical prostatectomy. The surgical specimens were first sliced thickly, and samples were then cut from suspect areas.

Tissue Sample Selection

Suspect areas were stained with H&E for histopathological examination in the surgery suite, and a thick shave of an adjacent section was immediately frozen at -80°C for RNA

Growth factor receptors		Various (metabolic enzymes...)	
CXCR4	Chemokine (C-X-C) receptor 4	A2M	Alpha-2-macroglobulin
DCC	Deleted in colorectal carcinoma	ABCB1	ATP-binding cassette (MDR1)
EDNBRB	Endothelin receptor type B	ACPP	Acid phosphatase, prostate
EGFR	EGF receptor (ERBB1)	ANPEP	Alanyl aminopeptidase
ERBB2	c-erbB-2	APOA1	Apolipoprotein A-1
ERBB3	c-erbB-3	AZGP1	Alpha-2-glycoprotein 1
ERBB4	c-erbB-4	BR3	Carboxylesterase 3
FGFR1	Fibroblast growth factor receptor 1	CHGA	Chromogranin A
FGFR2	Fibroblast growth factor receptor 2	CYP1B1	Cytochrome P450, subfamily I, polypeptide 1
FSHR	Follicle stimulating hormone receptor	CYP3A4	Cytochrome P450, subfamily IIIA, polypeptide 4
GPR54	Gprot-coupled receptor 54 (KISSR)	CYP19	Cytochrome P450, subfamily XIX (Aromatase)
GRPR	Gastrin-releasing peptide receptor	DNMT1	DNA methyltransferase 1
HTR2B	Serotonin 5 hydroxy-Trp receptor 2B	DNMT3A	DNA methyltransferase 3, alpha
IGF2R	IGF2 Receptor	DNMT3B	DNA methyltransferase 3, beta
IL6R	IL6 receptor	EEF1A1	Eukaryotic translation elongation factor 1 alpha 1
KIT	Stem cell factor receptor	EIF3S3	Eukaryotic translation initiation factor 3, subunit 3
LHCGR	LH/CG receptor	EPHX1	Epoxide hydrolase 1 microsomal
MET	HGF receptor	ERVWE1	Endogenous retroviral family W
NTRK1	Neurotrophic tyrosine kinase	FUT1	Fucosyl transferase 1
PDGFRA	PDGF receptor alpha	GSTP1	Glutathione S-transferase pi
PDGFRB	PDGF receptor beta	HDAC1	Histone deacetylase 1
PLAUR	uPA receptor	HLA-C	MHC, class I, C
PTCH	Patched homolog	HP	Haptoglobin
PTCH2	Patched homolog 2	HPN	Hepsin
RET	RET oncogene	KLK3	Kallikrein 3, (prostate specific antigen)
ROBO1	Roundabout, axon guidance receptor, homolog 1	KLK4	Kallikrein 4 (prostase)
ROBO2	Roundabout, axon guidance receptor, homolog 2	MECP2	Methyl CpG binding protein 2
DNA repair proteins		NOS1	NNOS, neuronal nitric oxide synthase 1
MLH1	MutL homolog 1	NOS2A	iNOS, inducible hepatocyte NOS2A
MSH2	MutS homolog 2	NOS3	ENOS, NOS3 (endothelial)
MSH3	MutS homolog 3	SCGB1A1	Secretoglobin, family 1A, member 1 (Uteroglobin)
MSH6	MutS homolog 6	SCGB1D2	Secretoglobin, family 1D, member 2
PMS1	PMS1 postmeiotic segregation increased 1	SRD5A2	Steroid-5-alpha-reductase
PMS2	PMS2 postmeiotic segregation increased 2	SIAT1	Sialyl transferase 1
RAD51	RAD51 homolog (RecA homolog)	SOD1	Superoxyde desmutase 1
Apoptosis		SOD2	Superoxyde desmutase 2
AKT1	AKT1 oncogene	PACE	Paired basic amino acid cleaving enzyme (Furin)
APAF1	Apoptotic protease activating factor 1	PCA3	Prostate cancer antigen 3
BAK1	BCL2 antagonist killer-1	STEAP	Six transmembrane epithelial antigen of the prostate
BAX	BCL2-associated X protein	TERT	Telomere reverse transcriptase
BCL2	B-Cell lymphoma 2 oncogene	TES	Testis derived transcript
BCL2L1	Long isoform, (BCL-XL)	TYMS	Thymidylate synthetase
BCL2L1	Short isoform (BCL-XS)		
BCLG	Apoptosis regulator BCL-G		
BID	BH3-interacting domain death agonist		
BIRC5	Survivin		
CASP3	Caspase 3		
CASP9	Caspase 9		
HCS	Cytochrome C		
PDCD8	Apoptosis-inducing factor (AIF)		
SMAC	Diablo/Smac protein		
Angiogenesis			
ANGPT1	Angiopoietin 1		
ANGPT2	Angiopoietin 2		
EFNB2	Ephrin-B2		
EPHA3	Ephrin receptor EphA3		
F2R	Thrombin receptor (TR); PAR1		
F3	Tissue factor (TF)		
FLT1	VEGF receptor 1 (VEGFR1)		
FLT4	VEGF receptor 3 (VEGFR3)		
HIF1A	Hypoxia-inducible factor 1 alpha		
KDR	VEGF receptor 2 (VEGFR2)		
MDK	Midkine (NEGF2)		
NRP1	Neuropilin 1		
PROK1	Prokineticin 1 (EG-VRGF)		
SERPINB5	Serin proteinase inhibitor (Maspin)		
TEK	TEK tyrosine kinase (TIE2)		
THBD	Thrombomodulin		
VEGF	VEGF-A		
VEGF165	VEGF-A isoform		
VEGFB	VEGF-B		
VEGFC	VEGF-C		
VEGFD	VEGF-D		
XLKD1	Lymph_vessel endoth receptor1 (LYVE1)		

Fig. 1 Continued.

Table 1 Clinical and histopathological features for 14 patients who underwent a radical prostatectomy for clinically prostate tumor

	Age ^a	PSA ^a	Pathological stage	Gleason score	Relapse ^b
T1	72	7.5	pT3 N0 M0	7	Yes
T5	65	19.7	pT2 N0 M0	6	Yes
T6	65	26.0	pT2 N0 M0	7	Yes
T8	73	10.5	pT2 N0 M0	7	No
T9	68	7.0	pT2 N0 M0	7	No
T20	69	5.2	pT2 N0 M0	7	No
T22	50	2.0	pT3 N0 M0	8	No
T25	60	8.0	pT3 N0 M0	7	Yes
T26	57	18.1	pT2 N0 M0	5	No
T41	54	10.0	pT2 N0 M0	7	Yes
T43	64	17.5	pT2 N0 M0	6	No
T46	67	8.8	pT3 N0 M0	5	No
T47	55	9.3	pT3 N0 M0	5	Yes
T49	71	8.2	pT3 N0 M0	7	Yes

^a At time of diagnosis.

^b At least 2 years of follow-up.

extraction and additional examination. This preselected tumor specimen was then sliced in the laboratory and again examined histologically. Samples were considered suitable for molecular studies when all examined epithelial cells were neoplastic. Malignant areas were carefully dissected with a scalpel, yielding a homogeneous cell population and avoiding dilution of tumor-specific genetic changes by nucleic acids from normal and reactive cells present in the same specimen. The histological diagnosis and clinical stage (based on the Tumor-Node-Metastasis system and Gleason score) were determined after surgery. Eight of the 14 selected tumors were stage pT2, and six were stage pT3. The Gleason score of the tumor area selected for RNA extraction was confirmed histologically by an experienced pathologist in the laboratory. The Gleason scores were 5–6 in five cases, 7 in eight cases, and 8 in one case.

With 2 years of follow-up, 7 of the 14 patients (three pT2 and four pT3) had progressed (as defined by two successive PSA values exceeding 0.2 ng/ml), whereas the other 7 patients (5 pT2 and 2 pT3) had not progressed.

The clinical characteristics of the 14 patients are shown in Table 1. Specimens of normal prostate tissue were obtained from 7 of these 14 patients who underwent radical prostatectomy and were used to determine basal target-gene mRNA expression. Normal-looking areas of each surgical specimen were examined histologically to confirm the absence of cancer cells and benign hyperplasia.

RNA Extraction and cDNA Synthesis

Total RNA was extracted from tissue specimens by using the acid-phenol guanidinium method (5). The quality of RNA extracts was determined by electrophoresis through agarose gels, staining with ethidium bromide, and visualization of the 18S and 28S RNA bands under UV light. cDNA was synthesized as described previously (6).

Real-Time RT-PCR

Theoretical Basis. Quantitative values are obtained from the Ct number at which the increase in signal associated with exponential growth of PCR products starts to be detected (using

PE Biosystems analysis software, according to the manufacturer's manual).

The precise amount of total RNA added to each reaction mix (based on absorbance) and its quality (*i.e.*, lack of extensive degradation) are both difficult to assess. We, therefore, also quantified *PPIA* (the peptidylprolyl isomerase A gene encoding cyclophilin A) and *RPLP0* (encoding the human acidic ribosomal phosphoprotein P0) transcripts as endogenous controls. *RPLP0* is also known as 36B4 and is widely used as an endogenous control for Northern blot analysis.

Results, expressed as N-fold differences in target gene expression relative to *PPIA* (or *RPLP0*) expression and termed “Ntarget,” were determined by the formula: $N_{target} = 2^{\Delta C_{t_{sample}}}$, where the ΔC_t value of the sample was determined by subtracting the average Ct value of the target gene from the average Ct value of the *PPIA* (or *RPLP0*) gene.

The Ntarget values of the prostate samples were subsequently normalized such that the mean of the seven normal prostate Ntarget values was 1.

Primers and PCR Consumables. Primers for *PPIA*, *RPLP0*, and the 291 target genes were chosen with the assistance of the Oligo 4.0 program (National Biosciences, Plymouth, MN). We performed Basic Local Alignment Search Tool (7) searches against dbEST, htgs, and nr (the nonredundant set of the GenBank, European Molecular Biology Laboratory, and DNA Data Bank of Japan database sequences) to confirm the total gene specificity of the nucleotide sequences chosen as primers and the absence of DNA polymorphisms. In particular, the primer pairs were selected to be unique relative to the sequences of closely related family member genes or corresponding retropseudogenes. Primer sets were also tested by PCR to ensure they yielded a single band on agarose gel, and PCR products were purified and sequenced to confirm primer specificity. To avoid amplification of contaminating genomic DNA, one of the two primers was placed at the junction between two exons or in a different exon (except for intronless genes). A primer pair lying in intron 12 of the albumin gene was used to check the DNA-free status of RNA samples (data not shown).

Moreover, genomic DNA was used as a template to confirm the RNA specificity of the primer set in each experiment.

For each set of primers, a no-template control and a no-reverse transcriptase control (reverse transcriptase-negative) assay, which produced negligible signals (usually Ct > 35), were used to confirm the absence of primer-dimer formation and genomic DNA contamination.

Standard Curve Method. A relative kinetic method was applied using standard curve. The latter was constructed with 4-fold serial dilutions of cDNA from a pool of normal prostate tissues. Standard curves were produced for the 291 target genes, *PPIA*, and *RPLP0*.

PCR Amplification. All PCR reactions were performed using an ABI Prism 7900 Sequence Detection System (Perkin-Elmer Applied Biosystems) and the SYBR Green PCR Core Reagents kit (Perkin-Elmer Applied Biosystems). The thermal cycling conditions comprised an initial denaturation step at 95°C for 10 min and 45 cycles at 95°C for 15 s and 65°C for 1 min.

Inclusion Criteria for Target Gene Assay. In a first step, prostate tumor mRNAs were mixed to obtain two prostate

tumor pools [one representative of patients without relapse 2 years after radical surgery ($n = 7$) and one with relapse ($n = 7$)] and a pool of paired normal prostate specimens.

Tissue samples were considered suitable when *PPIA* Ct values were between 17 and 19, reflecting an appropriate starting amount and quality of total RNA.

The mean Ct values of the prostate samples included in the pools were 18.17 ± 0.29 (patients without relapse), 18.00 ± 0.47 (patients with relapse), and 18.22 ± 1.45 (normal prostate samples).

Statistical Analysis

The distributions of mRNA levels were characterized on the basis of their medians and ranges. Relationships between the target genes and clinical and histological parameters were tested with the nonparametric Mann-Whitney *U* test. Differences were considered to be significant at confidence levels greater than 95% ($P < 0.05$).

To visualize the ability of a given molecular marker to discriminate two populations (in the absence of an arbitrary cutoff value), we summarized the data in a ROC curve (8). This curve plots sensitivity (true positives) on the Y axis against one specificity (false positives) on the X axis, considering each value as a possible cutoff. The AUC were calculated as a single measure for the discriminatory capacity of each molecular marker. When a molecular marker has no discriminatory value, the ROC curve lies close to the diagonal and the AUC is close to 0.5. When a molecular marker has strong discriminatory value, the ROC curve moves to the top left or bottom right corner and the AUC approaches 1 or 0.

Hierarchical clustering was performed using GeneANOVA software (9). The data sets were rank-transformed before analysis by the WARD method.

RESULTS

Gene Expression Profile in Clinically Localized Prostate Tumors. mRNA levels of 11 (3.8%) of the 291 target genes were very weak in both prostate tumor pools and in the normal prostate pool, being detectable but not reliably quantifiable ($Ct > 30$) by means of real-time quantitative RT-PCR with fluorescence SYBR Green methodology.

mRNA levels of each of the 291 genes were determined in the two prostate tumor pools and were compared with the mRNA levels of each gene in the normal prostate pool. The 88 genes displaying markedly altered expression (at least a 2-fold difference between at least one prostate tumor pool and the pool of normal prostate tissues) were selected for additional analysis in the 14 individual prostate tumors and seven paired normal prostate specimens.

Mean expression values obtained with the individual prostate tumors were very similar to those obtained with the corresponding pooled samples (data not shown). Median mRNA levels of 46 (52.3%) of these 88 genes differed significantly between the 14 prostate tumors and the seven normal prostate samples ($P < 0.005$, Mann-Whitney *U* test; Table 2). Five genes showed significantly higher expression in the tumor specimens, and 41 showed significantly reduced expression.

With regard to the five genes with significantly increased

expression, the ratio of the median value in the 14 prostate tumors and the median value in the seven normal prostate tissues ranged between 1.8 (*MMP9*) and 5.7 (*CDKN2A*). With regard to the 41 genes with significantly reduced expression, the ratio of the median value in the 14 prostate tumors and the median value in the seven normal prostate tissues ranged between 0.07 (*NRG1*) and 0.63 (*TYMS* and *UNC5C*).

The capacity of each of these 46 genes to discriminate between tumoral and normal prostate tissue was assessed by using the AUC-ROC method. The AUC values shown in Table 2 represent the capacity of each gene to discriminate between normal and tumoral prostate tissue. The *Ntarget* values indicated in Table 2 (calculated as described in "Materials and Methods") were based on the amount of the target message relative to the *PPIA* endogenous control, to normalize the amount and quality of total RNA; similar results were obtained by using a second endogenous RNA control, the *RPLP0* gene (also known as 36B4; data not shown).

The only associations between clinical and pathological features (e.g., age, serum PSA level at diagnosis, stage, and Gleason score) and the expression of individual target genes were between *ILK* and *F3* expression and the Gleason score ($P = 0.05$ and $P = 0.009$, respectively); increased *ILK* expression was associated with moderately or poorly differentiated tumors, and reduced *F3* expression was associated with poorly differentiated tumors.

Predictors of Clinical Outcome. With 2 years of follow-up, 7 of the 14 patients (three pT2 and four pT3) had progressed (as defined by two successive PSA values exceeding 0.2 ng/ml), whereas the other 7 patients (five pT2 and two pT3) had not progressed (Table 1).

The capacity of each gene to discriminate patients who relapsed from patients who did not relapse was estimated by the AUC-ROC method. By combining the two genes with the AUC-ROC values closest to 0 (*XLKDI/LYVE1* and *CGA*; 0.061 and 0.143, respectively) and the two genes with the AUC-ROC values closest to 1.0 (*F2R/PAR1* and *BCL-G*; 0.878 and 0.714, respectively), we obtained a four-gene model that discriminated perfectly between the seven patients with and the seven patients without relapse, independently of stage and grade. *XLKDI/LYVE1* and *CGA* expression was significantly lower ($P < 0.05$, Mann-Whitney *U* test) in patients who relapsed than in patients who did not relapse (median values: 0.06 versus 0.24 and 0.36 versus 3.55, respectively), whereas *BCL-G* and *F2R/PAR1* expression was significantly higher (1.04 versus 0.48 and 1.27 versus 0.58, respectively; data not shown).

The gene clusters are shown as dendograms (Fig. 2), in which line length and branching reflect the relatedness of the samples according to the expression of the four genes.

DISCUSSION

We studied the mRNA expression of 291 genes involved in pathways (e.g., cell cycling, signal transduction, apoptosis, angiogenesis, and metastasis) that are known to be dysregulated in solid tumors, including CaP.

Eighty-eight genes showed at least a 2-fold difference in expression between pooled prostate tumors and pooled normal prostate tissues. The expression level of these 88 genes was then

Table 2 List of the significantly altered expressed genes in prostate tumors compared with normal prostate specimens

Genes	Normal prostate specimens ($n = 7$) ^a	Prostate tumors ($n = 14$)	Ratio	ROC-AUC
<i>XDL1</i> (<i>LYVE1</i>) ^b	0.93 ^c	0.11 ^d	0.116	0.000
<i>ILK</i>	0.97	0.46	0.474	0.009
<i>DCC</i>	0.97	0.12	0.122	0.013
<i>NRG1</i>	0.87	0.06	0.072	0.017
<i>BMP7</i>	1.02	0.35	0.344	0.024
<i>NOS1</i>	1	0.09	0.095	0.025
<i>SRD5A2</i>	1.12	0.16	0.144	0.032
<i>SERPINB5</i> (Maspin)	1.04	0.11	0.103	0.037
<i>FGR2IIIB</i>	0.88	0.25	0.282	0.037
<i>ITG3B</i>	0.99	0.39	0.393	0.041
<i>NTN1</i> (netrin-1)	0.95	0.25	0.267	0.045
<i>GSTP1</i> (GST π)	1.04	0.35	0.336	0.049
<i>ITGA5</i>	0.83	0.24	0.285	0.053
<i>GRO1</i>	1.01	0.22	0.218	0.055
<i>AREG</i>	1.15	0.16	0.135	0.063
<i>PROK1</i>	1	0.12	0.124	0.067
<i>SPARC-LIKE</i>	0.98	0.6	0.611	0.070
<i>IGB4</i>	0.99	0.29	0.296	0.072
<i>CALD1</i>	1	0.39	0.395	0.072
<i>PIA2</i>	0.79	0.17	0.21	0.075
<i>THBD</i> (thrombomodulin)	0.91	0.28	0.309	0.077
<i>ROBO 1</i>	0.87	0.34	0.391	0.078
<i>GJA1</i> (connexin 43)	1.02	0.49	0.48	0.100
<i>MMP14</i>	0.94	0.51	0.54	0.105
<i>CD44</i>	1.02	0.45	0.441	0.117
<i>NOS2A</i>	0.91	0.23	0.259	0.124
<i>SIAT</i>	0.93	0.38	0.41	0.130
<i>SFN</i> (Stratifin)	1.25	0.22	0.177	0.133
<i>TYMS</i>	0.86	0.55	0.632	0.148
<i>CD13</i>	0.65	0.06	0.087	0.149
<i>CXR4</i>	0.96	0.46	0.479	0.157
<i>CYP1B1</i>	0.97	0.49	0.505	0.158
<i>GRP</i>	0.96	0.17	0.177	0.165
<i>CAV1</i>	1.01	0.28	0.281	0.193
<i>CHGA</i>	0.78	0.12	0.154	0.200
<i>RET</i>	1.18	0.23	0.198	0.208
<i>ROBO 2</i>	0.87	0.47	0.540	0.212
<i>UNC5C</i>	0.84	0.53	0.631	0.221
<i>CDKN2B</i> (p15)	0.94	0.49	0.521	0.222
<i>SLIT 3</i>	0.84	0.48	0.571	0.255
<i>EDNRB</i> (ETB)	0.78	0.48	0.615	0.273
<i>COL1A1</i>	0.94	1.89	2.004	0.761
<i>MMP9</i>	1.08	1.96	1.812	0.785
<i>PCA3</i> (DD3)	0.99	2.18	2.202	0.829
<i>GRPR</i>	1	3.14	3.143	0.885
<i>CDKN2A</i> (p16)	0.89	5.09	5.686	0.969

^a Mann-Whitney *U* test.^b Locus Link (Usual name).^{c,d} Numbers represent *Ntarget* (see "Materials and Methods") medians of normal prostate specimens and prostate tumors, respectively.

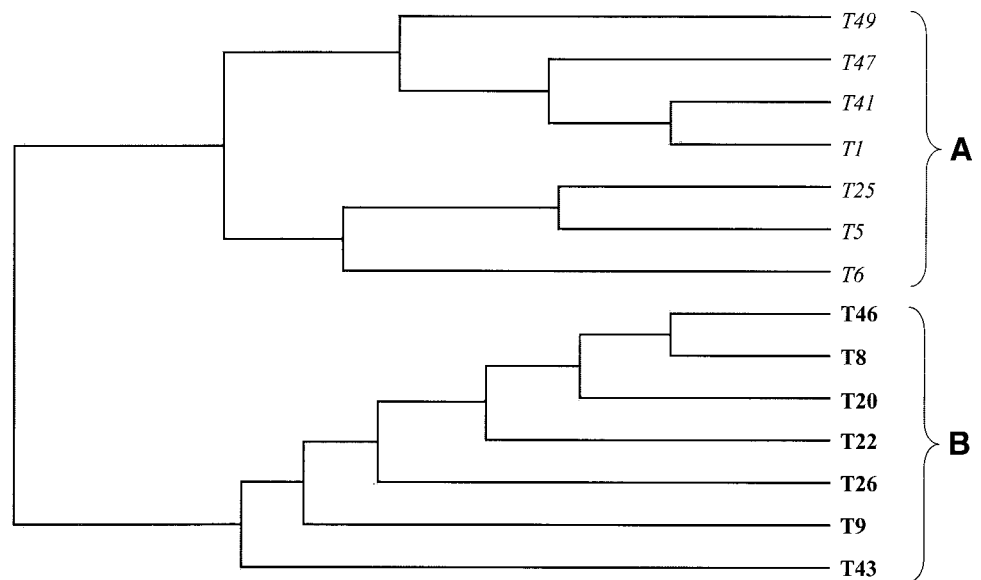
studied individually in 14 prostate tumors and seven normal prostate specimens. Analysis of the expression level of these 88 genes in each sample further allowed us to check for potential heterogeneity within each pool. Mean values calculated for individual prostate tumors were very close to the value obtained for the corresponding pooled samples (data not shown), indicating that the initial evaluation based on pooled samples was reliable. The expression of 5 of the 88 selected genes was significantly increased, whereas that of 41 genes was significantly decreased (Table 2). It is noteworthy that the proliferative marker *MKI67* had no discriminatory value, the ROC curves lying close to the diagonal and the AUC value being close to 0.5

(AUC-ROC, 0.479; data not shown), suggesting that the dysregulation of the 46 target genes in prostate tumors was not caused by the high proliferative activity of cancer cells.

The gene expression pattern in prostate tumors was related to: (a) complex physiological properties (e.g., angiogenesis and invasion); (b) the activity of specific signaling pathways (e.g., *DCC*, *NTN1*, and *ROBO*); and (c) cell specificity (e.g., stroma-dependent expression of growth factors).

First, most of the dysregulated genes belonged to the ECM and ECM-remodeling categories and were involved in angiogenesis (e.g., *XLKD1/LYVE1*, *PROK1*, *SERPINB5/Maspin*, and *THBD*). The MMP gene *MMP9* was overexpressed in the tu-

Fig. 2 Hierarchical clustering was applied to 14 clinically localized prostate tumors on the basis of expression data from four genes (*XLKDI/LYVE1*, *CGA*, *F2R/PAR1*, and *BCL-G*). These four genes were selected from a total of 291 genes by the AUC-ROC test described in "Materials and Methods." **A**, patients with relapse. **B**, patients who remained relapse free for at least 2 years after surgery.



mors, whereas all of the other genes (ECM, ECM-remodeling, and angiogenesis dysregulated genes: *MMP14*, *ITGA5*, *ITGB4*, *ITGB3*, *XLKDI/LYVE1*, *PROK1*, *SERPINB5/Maspin*, and *THBD*) were underexpressed. Except for *CDKN2A*, no genes involved in cell cycling, DNA synthesis, or gene transcription activities related to the highly proliferative status of cancer cells were dysregulated. Similarly, no genes involved in apoptotic pathways were significantly dysregulated. However, the anti-apoptotic gene *BIRC5/Survivin* was expressed about 1.6 times more strongly in the tumors than in the normal prostate tissues (data not shown).

Second, several key genes in axon guidance and cell migration were underexpressed in prostate tumors, including *NTN1/netrin-1*, the chemoattractant gene and its receptor *DCC* (deleted in colorectal cancer), and *SLIT3* and its *ROBO* (Roundabout) receptors. These genes might, therefore, be involved in the chemotactic behavior of CaP cells.

Finally, most of the growth factor genes dysregulated in prostate tumors were down-regulated (*AREG*, *NRG1*, *BMP7*, *GRO1*, and so forth), possibly because of the stroma-dependent nature of their expression.

Some of the genes found to be dysregulated here have already been forwarded as cancer biomarkers or mediators of prostate carcinogenesis. For example, *PCA3* (also known as *DD3*) has already been shown to be overexpressed in prostate tumors (10) and is a very sensitive and specific marker of this malignancy (11); *GRPR* (gastrin-releasing peptide receptor), which has high affinity for gastrin-releasing peptide and bombesin, has also been shown to be overexpressed (12), and therapeutic approaches based on bombesin receptor antagonists and cytotoxic bombesin analogues have been considered in CaP (13). We also found a 9.7-fold decrease in the expression of *SERPINB5/maspin*, in keeping with the role of the corresponding protein as an angiogenesis inhibitor (14) that acts at the cell membrane to inhibit the invasiveness and motility of prostatic cancer cells (15).

We identified some other genes or their products as potential therapeutic targets in CaP.

MMP9 was overexpressed, and synthetic inhibitors of MMPs have therapeutic efficacy in various cancers. Recently, a novel inhibitor, Ro 28-2653, with high selectivity for *MMP9*, showed promise in patients with CaP (16).

CDKN2A exon 1 α (p16) transcripts were overexpressed in prostate tumors; indeed, 8 (57%) of 14 prostate tumors displayed increased expression of p16*CDKN2A*, varying from 2- to 10-fold higher than normal prostate tissues. In contrast, a decrease in p16*CDKN2A* expression was found in three prostate tumors (data not shown). The product of this gene is a cyclin-dependent kinase inhibitor that functions as a cell growth regulator controlling cell cycle G₁ progression through engagement of the Rb-cdk4/6-cyclin D pathway (17). p16*CDKN2A* overexpression has already been described in solid tumors including CaP (18). An altered *RBI* axis could trigger p16*CDKN2A* overexpression in certain systems. However, we found no association, at the mRNA level, between p16*CDKN2A* and *RBI* or other cell cycle regulator expression.

It is of note that the p14^{ARF} product encoded by this gene, through an alternate open reading frame, was expressed 1.6 times more strongly in the tumors than in the normal prostate tissues (data not shown).

Other interesting candidate targets are key genes in axon guidance and cell migration in the central nervous system, such as the secreted proteins netrin-1 and slit3.

We then analyzed the prostate tumor gene expression signature according to tumor recurrence. Recurrence is a major problem in this setting, because 30% of men undergoing radical prostatectomy for localized tumors eventually relapse, and none of the current indicators of progression (stage and grade at diagnosis) can predict outcome (Table 1). There is, thus, an urgent need for robust prognostic markers capable of identifying patients at risk of relapse after radical surgery.

In this study, the patients were all assessable with respect

to recurrence after surgery; seven patients relapsed (defined as two successive PSA values >0.2 ng/ml), and seven remained relapse free for at least 2 years. We used the AUC-ROC test to assess the prognostic value of each gene in terms of relapse. A four-gene model based on the two genes with the AUC values closest to 0 (*XLKD1/LYVE1* and *CGA*) and the two genes with the AUC values closest to 1 (*F2R/PAR1* and *BCL-G*) perfectly discriminated between the seven patients who relapsed and the seven patients who did not relapse after 2 years of follow-up (Fig. 2). *XLKD1/LYVE1* and *F2R/PAR1* encode angiogenic factors *BCL-G*, a proapoptotic factor, and *CGA*, a growth factor.

CGA is the α -subunit of the human glycoprotein hormone chorionic gonadotropin. *CGA* was overexpressed in patients who did not relapse, in keeping with our previous work showing that *CGA* is a specific *ER α* -responsive gene in CaP and that its overexpression may be associated with a good prognosis in CaP (19) as in breast cancer (20).

XLKD1/LYVE-1 is an endocytic receptor for hyaluronan in lymphatic endothelium (21). The functional role of *XLKD1/LYVE-1* in lymphatic vessels, and its use as a marker of tumor lymphangiogenesis, are important areas of investigation. In our study, the association between low *XLKD1/LYVE-1* expression and poor outcome is in keeping with the known function of this gene; indeed, *XLKD1/LYVE-1*-positive structures have been observed in lung tumor margins but not within the mass of such tumors (22). Moreover, negative intratumoral *XLKD1/LYVE-1* staining does not rule out metastasis (23), suggesting that functional lymphatics in the tumor margins are sufficient for lymphatic metastasis (22).

We also found that increased *F2R/PAR1* expression was associated with tumor recurrence. This coagulation factor II (thrombin) receptor is involved in regulating the thrombotic response. Thrombin promotes angiogenesis by enhancing vascular endothelial growth factor synthesis and inducing its secretion and has already been implicated in prostate tumorigenesis and metastasis (24).

Last, overexpression of *BCL-G*, encoding a *BCL2* family protein, has been shown to induce apoptosis in COS-7 cells (25). However, little is known about the expression of this gene in tumor samples, and *BCL-G* has not been linked previously to clinical outcome.

Our results indicate that although *F2R/PAR1* and *BCL-G* overexpression are associated with poor outcome, optimal outcome prediction is obtained by their combination with genes, such as *CGA*, that are associated with good outcome. The resulting four-gene model was perfectly predictive of tumor recurrence, independently of tumor stage and grade. It is noteworthy that *F3* and *ILK*, the expression of which correlates with the Gleason score, a current prognostic marker, were excluded from this model.

In conclusion, our data identify potential new therapeutic targets in CaP and show that gene expression profiling can be used as a predictor of outcome. Routine clinical use of genomics-based outcome predictors must await confirmation in larger, independent data sets.

REFERENCES

1. Parker, S. L., Tong, T., Bolden, S., and Wingo, P. A. Cancer statistics, 1997. *CA Cancer J. Clin.*, **47**: 5–27, 1997.

2. Dhanasekaran, S. M., Barrette, T. R., Ghosh, D., Shah, R., Varambally, S., Kurachi, K., Pienta, K. J., Rubin, M. A., and Chinnaiyan, A. M. Delineation of prognostic biomarkers in prostate cancer. *Nature (Lond.)*, **412**: 822–826, 2001.

3. Luo, J. H., Yu, Y. P., Cieply, K., Lin, F., DeFlavia, P., Dhir, R., Finkelstein, S., Michalopoulos, G., and Becich, M. Gene expression analysis of prostate cancers. *Mol. Carcinog.*, **33**: 25–35, 2002.

4. Singh, D., Febbo, P. G., Ross, K., Jackson, D. G., Manola, J., Ladd, C., Tamayo, P., Renshaw, A. A., D'Amico, A. V., Richie, J. P., Lander, E. S., Loda, M., Kantoff, P. W., Golub, T. R., and Sellers, W. R. Gene expression correlates of clinical prostate cancer behavior. *Cancer Cells*, **1**: 203–209, 2002.

5. Chomczynski, P., and Sacchi, N. Single-step method of RNA isolation by acid guanidinium thiocyanate-phenol-chloroform extraction. *Anal. Biochem.*, **162**: 156–159, 1987.

6. Latil, A., Bieche, I., Vidaud, D., Lidereau, R., Berthon, P., Cussenot, O., and Vidaud, M. Evaluation of androgen, estrogen (*ER α* and *ER β*), and progesterone receptor expression in human prostate cancer by real-time quantitative reverse transcription-polymerase chain reaction assays. *Cancer Res.*, **61**: 1919–1926, 2001.

7. Altschul, S. F., Gish, W., Miller, W., Myers, E. W., and Lipman, D. J. Basic Local Alignment Search Tool. *J. Mol. Biol.*, **215**: 403–410, 1990.

8. Hanley, J. A., and McNeil, B. J. The meaning and use of the area under a receiver operating characteristic (ROC) curve. *Radiology*, **143**: 29–36, 1982.

9. Didier, G., Brezellec, P., Remy, E., and Henaut, A. GeneANOVA—gene expression analysis of variance. *Bioinformatics*, **18**: 490–491, 2002.

10. Bussemakers, M. J., van Bokhoven, A., Verhaegh, G. W., Smit, F. P., Karthaus, H. F., Schalken, J. A., Debruyne, F. M., Ru, N., and Isaacs, W. B. DD3: a new prostate-specific gene, highly overexpressed in prostate cancer. *Cancer Res.*, **59**: 5975–5979, 1999.

11. de Kok, J. B., Verhaegh, G. W., Roelofs, R. W., Hessels, D., Kiemene, L. A., Aalders, T. W., Swinkels, D. W., and Schalken, J. A. DD3(PCA3), a very sensitive and specific marker to detect prostate tumors. *Cancer Res.*, **62**: 2695–2698, 2002.

12. Markwalder, R., and Reubi, J. C. Gastrin-releasing peptide receptors in the human prostate: relation to neoplastic transformation. *Cancer Res.*, **59**: 1152–1159, 1999.

13. Pinski, J., Schally, A. V., Halmos, G., and Szepeshazi, K. Effect of somatostatin analog RC-160 and bombesin/gastrin releasing peptide antagonist RC-3095 on growth of PC-3 human prostate-cancer xenografts in nude mice. *Int. J. Cancer*, **55**: 963–967, 1993.

14. Zhang, M., Volpert, O., Shi, Y. H., and Bouck, N. Maspin is an angiogenesis inhibitor. *Nat. Med.*, **6**: 196–199, 2000.

15. Sheng, S., Carey, J., Seftor, E. A., Dias, L., Hendrix, M. J., and Sager, R. Maspin acts at the cell membrane to inhibit invasion and motility of mammary and prostatic cancer cells. *Proc. Natl. Acad. Sci. USA*, **93**: 11669–11674, 1996.

16. Lein, M., Jung, K., Ortel, B., Stephan, C., Rothaug, W., Juchem, R., Johannsen, M., Deger, S., Schnorr, D., Loening, S., and Krell, H. W. The new synthetic matrix metalloproteinase inhibitor (Roche 28–2653) reduces tumor growth and prolongs survival in a prostate cancer standard rat model. *Oncogene*, **21**: 2089–2096, 2002.

17. Kamb, A., Gruis, N. A., Weaver-Feldhaus, J., Liu, Q., Harshman, K., Tavtigian, S. V., Stockert, E., Day, R. S., III, Johnson, B. E., and Skolnick, M. H. A cell cycle regulator potentially involved in genesis of many tumor types. *Science (Wash. DC)*, **264**: 436–440, 1994.

18. Lee, C. T., Capodice, P., Osman, I., Fazzari, M., Ferrara, J., Scher, H. I., and Cordon-Cardo, C. Overexpression of the cyclin-dependent kinase inhibitor p16 is associated with tumor recurrence in human prostate cancer. *Clin. Cancer Res.*, **5**: 977–983, 1999.

19. Bieche, I., Latil, A., Parfait, B., Vidaud, D., Laurendeau, I., Lidereau, R., Cussenot, O., and Vidaud, M. *CGA* gene (coding for the alpha subunit of glycoprotein hormones) overexpression in *ER α* -positive prostate tumors. *Eur. Urol.*, **41**: 335–341, 2002.

20. Bieche, I., Parfait, B., Nogues, C., Andrieu, C., Vidaud, D., Spyrtos, F., Lidereau, R., and Vidaud, M. The CGA gene as new predictor of the response to endocrine therapy in ER α -positive postmenopausal breast cancer patients. *Oncogene*, 20: 6955–6959, 2001.
21. Prevo, R., Banerji, S., Ferguson, D. J., Clasper, S., and Jackson, D. G. Mouse LYVE-1 is an endocytic receptor for hyaluronan in lymphatic endothelium. *J. Biol. Chem.*, 276: 19420–19430, 2001.
22. Padera, T. P., Kadambi, A., di Tomaso, E., Carreira, C. M., Brown, E. B., Boucher, Y., Choi, N. C., Mathisen, D., Wain, J., Mark, E. J., Munn, L. L., and Jain, R. K. Lymphatic metastasis in the absence of functional intratumor lymphatics. *Science (Wash. DC)*, 296: 1883–1886, 2002.
23. Mandriota, S. J., Jussila, L., Jeltsch, M., Compagni, A., Baetens, D., Prevo, R., Banerji, S., Huarte, J., Montesano, R., Jackson, D. G., Orci, L., Alitalo, K., Christofori, G., and Pepper, M. S. Vascular endothelial growth factor-C-mediated lymphangiogenesis promotes tumour metastasis. *EMBO J.*, 20: 672–682, 2001.
24. Huang, Y. Q., Li, J. J., Hu, L., Lee, M., and Karpatkin, S. Thrombin induces increased expression and secretion of VEGF from human FS4 fibroblasts, DU145 prostate cells and CHRF megakaryocytes. *Thromb. Haemost.*, 86: 1094–1098, 2001.
25. Guo, B., Godzik, A., and Reed, J. C. Bcl-G, a novel pro-apoptotic member of the Bcl-2 family. *J. Biol. Chem.*, 276: 2780–2785, 2001.

Clinical Cancer Research

Gene Expression Profiling in Clinically Localized Prostate Cancer: A Four-Gene Expression Model Predicts Clinical Behavior

Alain Latil, Ivan Bièche, Laurent Chêne, et al.

Clin Cancer Res 2003;9:5477-5485.

Updated version Access the most recent version of this article at:
<http://clincancerres.aacrjournals.org/content/9/15/5477>

Cited articles This article cites 24 articles, 11 of which you can access for free at:
<http://clincancerres.aacrjournals.org/content/9/15/5477.full#ref-list-1>

Citing articles This article has been cited by 5 HighWire-hosted articles. Access the articles at:
<http://clincancerres.aacrjournals.org/content/9/15/5477.full#related-urls>

E-mail alerts [Sign up to receive free email-alerts](#) related to this article or journal.

Reprints and Subscriptions To order reprints of this article or to subscribe to the journal, contact the AACR Publications Department at pubs@aacr.org.

Permissions To request permission to re-use all or part of this article, use this link
<http://clincancerres.aacrjournals.org/content/9/15/5477>.
Click on "Request Permissions" which will take you to the Copyright Clearance Center's (CCC) Rightslink site.